

PLYWOODS OF NORTHEAST ARGENTINIAN WOODS AND SOYBEAN PROTEIN-BASED ADHESIVES: RELATIONSHIP BETWEEN MORPHOLOGICAL ASPECTS OF VENEERS AND SHEAR STRENGTH VALUES

*E. S. Nicolao*¹

<https://orcid.org/0000-0003-2549-9533>

*S. Monteoliva*²

<https://orcid.org/0000-0002-8679-7633>

*E. M. Ciannamea*¹

<https://orcid.org/0000-0001-6982-1550>

P. Stefani^{1,*}

<https://orcid.org/0000-0002-8140-4415>

ABSTRACT

Three-ply plywoods were produced using pine and *Eucalyptus* northeast Argentinian woods. A no-added formaldehyde biobased-adhesive was used for assembly, based on chemically modified soy protein concentrate. In this work we focused on the relationship between bonding quality parameters of the plywoods and the morphology of the glued line. Wood characteristics such as contact angle, roughness, density and moisture content were measured prior to plywood assembly. Bonding quality parameters (percentage of wood failure and shear strength) of the plywood were measured according to Argentinean standard IRAM 9562 (2006) and the results were evaluated with respect to microscopic observations of the glue joint. *Eucalyptus* wood was suitable for plywood interior condition applications, while pine barely exceeded the standards imposed by the norm.

Keywords: Biogenic adhesive, bonding quality, mechanical properties, plywood, wood taxonomy.

INTRODUCTION

Increased demand of natural resources, mostly wood, have led to the development of new alternative materials for countless industrial applications. In particular, veneer-based products, especially plywoods, which are mostly used for structural applications, are important due to their versatile use and lower cost in comparison to other composite materials (Buddi *et al.* 2017). According to FAO data, the world production of veneer sheets and plywood in 2018 was 163 million m³ and it is expected to rise in the following years (FAO 2018).

The following work focuses especially on *Eucalyptus* (EU) and pine (PI) plywoods using a soy protein concentrate (SPC) based adhesive for the following reasons.

¹National University of Mar del Plata, Research Institute of Materials Science and Technology (INTEMA), National Scientific and Technical Research Council (CONICET), Mar del Plata, Argentina.

²National University of La Plata, Agricultural and Forest Sciences Faculty, INFIVE-CONICET Mar del Plata, Argentina.

*Corresponding author: pmstefan@fi.mdp.edu.ar

Received: 23.12.2020 Accepted: 21.09.2021

Argentina's forest resource is made up of both exotic and native species. Current environmental policies and regulations linked to the preservation of natural forests and the increasing demand for wood and its derivatives, have promoted the sustainable production of cultivated forest. There are approximately 1180000 hectares of cultivated forests of PI and EU species, 25 % corresponding to EU concentrating in the Mesopotamia area of Argentina, which ensures the local availability of resources (Nicolao *et al.* 2020). Furthermore, the forestry sector can still be explored if its full potential is taken into account (Pizzi 2006).

Anatomically, differences between species are related to cell structure: that is the types, sizes, ratios between cell walls and lumens width, pits, and arrangements of different cells that comprise the wood. These differences make woods heavy or light, stiff or flexible, hard or soft (Piter *et al.* 2007, Nordqvist *et al.* 2013).

The structure of softwoods is relatively simple compared to hardwoods. The axial or vertical system is composed mostly (95 % - 98 %) of axial tracheids for water conduction and mechanical support. Hardwoods, on the other hand, have perforated tracheary elements (vessels elements) for water conduction (10 % - 20 %), fibres (60 % - 70 %) for mechanical support and parenchyma (5 % - 10 %), as part of the axial system (Frihart and Hunt 2010).

Moreover, its structure not only depends on the specie being analyzed (hardwood or softwood in large terms) but also depends on subtler characteristics, such as percent of early or late wood within the tree-ring in the growing season, which gives variations in the ratio between the width of the lumen and the thickness of the cell wall (Bulfe and Fernandez 2017). Changes from early to late wood may be more or less subtle within in the same ring depending the specie, noticing that these change are important for pine (Denne 1989), and not for *Eucalyptus* wood. Understanding all this differences in cellular architecture allows insight to the realm of wood as an engineering material.

Wood is composed of cellulose, lignin, hemicelluloses, and minor amounts (usually less than 10 %) of extractives materials contained in a cellular structure.

Alternative adhesives have emerged to contrast the negative effects of urea-formaldehyde, the main adhesive used in wood composite materials, since formaldehyde has been classified as a human carcinogen and is obtained from non-renewable resources (Ghahri *et al.* 2021). Regulations on formaldehyde emissions (Salthammer *et al.* 2010) have become a driving force towards the search of new adhesive formulations based on sustainable raw materials such as starch, natural polyphenols, carbohydrates and proteins (Pizzi 2006, Frihart and Birkeland 2014). Numerous works have been done so far with respect to natural adhesives including protein (Mo and Sun 2013, Nordqvist *et al.* 2013), tannin (Stefani *et al.* 2008, Xi *et al.* 2020), tamarind (Buddi *et al.* 2017), and lignin-based adhesives (Ang *et al.* 2019) to name some of them. In particular, soy-based adhesives are a promising alternative. They are produced from renewable agricultural resources, are environmentally friendly and are less likely to cause health problems (Nicolao *et al.* 2020). Argentina is the third largest producer of soybeans in the world (54 million tones 2019/2020) (ASA 2020), so the use of adhesives based on this crop is also attractive from the point of view of taking advantage of the own country's resources. Our research group has made numerous studies in this field, involving from the development of soy protein concentrate (SPC) based adhesives to its application in plywood and rice husk based boards (Ciannamea *et al.* 2010, Ciannamea *et al.* 2012, Ciannamea *et al.* 2017, Nicolao *et al.* 2020). According to our previous research, particleboards based on rice husk and SPC treated with boric acid showed the best mechanical and water resistance properties, in comparison with other studied chemical treatments, as urea, citric acid or alkali (Ciannamea *et al.* 2012, Chalapud *et al.* 2020). Boric acid can react with OH from side groups of proteins, carbohydrates in soybean concentrate and BSPC can also react with OH groups present in wood, favored by hot pressing conditions (Ciannamea *et al.* 2012).

In addition to all the possible variations in wood structure named above, plywoods are materials that involve joints between veneer faces. These joints provide even more discontinuities in the material that must be studied and paid attention to. Joints under load must transfer stress from component to component through the interphase region, thus, the characteristics of the bond will impact on the performance of the plywood (Kamke and Lee 2007, Piter *et al.* 2007). Making a chain-link analogy of a union between woods, the bond will be as good as the weakest link in the chain (Marra 1992). An expected plywood performance would be that in which the weakest link is located inside the wood meaning that mechanical performance should be limited by wood resistance and not by the adhesion itself. Thus, one of the standards used in plywood manufacture, IRAM 9562 (2006), establishes not only shear strength tolerances but also wood failure percentage tolerances (WF %) as a quality criteria.

Several adhesion models, with their focus on surface interactions between the adhesive and the adherent, have been proposed over the years for most adherents; however, they have failed when applied to wood composites mainly due to wood variability explained before (Jakes *et al.* 2019). Numerous studies have focused on understanding what happens at the interface between plywood veneers (Chandler *et al.* 2005, Frihart 2005, Piter *et al.* 2007, Jakes *et al.* 2019). Understanding the differences between the species used, in morphological and morphometric terms, allows predicting, in a certain way, the behavior of a glued joint.

In this work we employed a previously developed no-added formaldehyde adhesive based on chemically treated SPC to obtain EU and PI plywoods. We specially focused in the relationship between bonding quality parameters of the plywoods (measured according to IRAM 9562 (2006) standard) and the microscopic observations of the glued joints. It is expected that the morphology/morphometry of each one of the species used and the degree of penetration of the adhesive plays a fundamental role in the quality of the gluing.

MATERIALS AND METHODS

Materials

Soybean protein concentrate (SPC, Solcom S 110) was provided by Cordis SA (Villa Luzuriaga, Buenos Aires, Argentina). SPC presented 7 % moisture, 69 % protein, 1 % fat, 3 % fibers, 5 % ash and about 15 % non-starch polysaccharides (mainly cellulose, non cellulose polymers and pectin polysaccharides) as mean composition and has an average particle size that could pass through a 100 mesh. Veneers of EU (*Eucalyptus grandis*) and PI (*Pinus taeda*), from specimens cultivated in northeast region of Argentina, were supplied by Forestadora Tapebicua SA. The age of the PI veneer's logs was 19 years, while for EU it was only 12 years old. Veneers were carefully inspected and selected avoiding major defects such as knots or cracks. Sodium hydroxide (NaOH, Anedra, Argentina), diiodomethane, Glycerol (Anedra, Argentina, 99 % purity) and safranin were purchased from the Sigma Chemical Co. (St. Louis, MO).

Methods

Adhesive preparation

Adhesive was prepared according previous works (Ciannamea *et al.* 2012) by dispersing SPC in a 0,3 % w/v boric acid (BA) solution at a ratio 1:10 (SPC:BA solution) under stirring ($500 \text{ rad}\cdot\text{s}^{-1}$) at room temperature for 2 h. The adhesive was lyophilized for 72 hours and stored in a dry environment for later use (BSPC stands boric modified SPC).

Rheological study of the adhesive

The apparent viscosity of the SPC-based adhesives was measured with an Anton Paar MCR 301 rheometer (Graz, Austria) at $25 \text{ }^\circ\text{C} \pm 0,2 \text{ }^\circ\text{C}$ over a shear rate range of 1 s^{-1} to 750 s^{-1} . Lyophilized adhesives were dispersed in distilled water in weight relations of 1:4, 1:5, 1:6, 1:7 and 1:10 (lyophilized BSPC adhesive:water ratio), mixed for 10 min, and transferred into the sample holder of the viscometer.

Veneers and plywoods preconditioning

EU and PI veneers, as well as plywoods, were kept 7 days in an environmental chamber at $65 \% \pm 5 \%$ relative humidity and $20 \text{ }^\circ\text{C} \pm 2 \text{ }^\circ\text{C}$ before carrying out any test. All veneers samples were sanded within 24 hours before any test or plywood assembly with an abrasive paper until achieving an average surface roughness R_a of $7 \text{ } \mu\text{m} \pm 2 \text{ } \mu\text{m}$.

Veneer characterization

Density and humidity

Density of veneers was determined following norm IRAM 9544 (1973) on samples previously stabilized in environmental chamber. Weight was measured gravimetrically using an analytical balance (Ohaus, $\pm 0,0001$). The dimension of the testing samples was measured with a digital caliper (Asimeto model 307-06-4, Germany, $0-150 \text{ mm} \pm 0,01 \text{ mm}$) and thickness was measured using a digital micrometer (Asimeto model IP65, Germany, $0-25 \text{ mm} \pm 0,01 \text{ mm}$) at eight random locations of each specimen.

The same samples were dried at $102 \text{ }^\circ\text{C} \pm 3 \text{ }^\circ\text{C}$ to constant weight in a convection oven in order to calculate moisture content according to IRAM 9532 (1993).

Surface energy and contact angle

The free surface energy was calculated by means of Owens-Wendt method. Following the description reported by Vazquez et al (Vázquez *et al.* 2011), it is possible to calculate the polar and dispersive components of the surface energy by means of the Equation 1:

$$\frac{0,5\gamma_{LV}(1+\cos\theta)}{\sqrt{\gamma_{LV}^d}} = \sqrt{\gamma_{SV}^p} \left(\frac{\gamma_{LV}^p}{\gamma_{LV}^d} \right)^{\frac{1}{2}} + \sqrt{\gamma_{SV}^d} \quad (1)$$

Where θ the contact angle formed between the liquid and the solid and γ_{LV}^p and γ_{LV}^d are the polar and dispersive components of the solid's free surface respectively. Linearizing Equation 1, energy can be obtained as the slope and ordinate at the origin, respectively, whose sum results in the total value of the free surface energy.

The polar component γ_{LV}^p and dispersive component γ_{LV}^d of each of the liquids used are well known values reported in literature (Scheikl and Dunky 1998, Vázquez *et al.* 2011). These liquids are: distilled water ($\gamma_{LV}^p=51 \text{ mN}\cdot\text{m}^{-1}$, $\gamma_{LV}^d=21,8 \text{ mN}\cdot\text{m}^{-1}$), glycerol ($\gamma_{LV}^p=30 \text{ mN}\cdot\text{m}^{-1}$, $\gamma_{LV}^d=34 \text{ m}\cdot\text{N}\cdot\text{m}^{-1}$) and diiodomethane ($\gamma_{LV}^p=0 \text{ mN}\cdot\text{m}^{-1}$, $\gamma_{LV}^d=50,8 \text{ mN}\cdot\text{m}^{-1}$). Is calculated by means of the following approach. The wetting process can be divided into two wetting phases: an extension phase in which the wetting speed ($d\theta/dt$) is relatively fast and a penetration stage, in which the rate of change of the contact angle is almost constant (Wolkenhauer *et al.* 2009, Vázquez *et al.* 2011). Equilibrium contact angle θ is considered at the point where $d\theta/dt$ becomes constant.

Ten measurements were made in PI and EU samples employing a 7 l drop. Measurements were made perpendicular to the direction of the wood fibers. A Rame-Hart contact angle goniometer equipment (New Jersey, USA) was used which can record $15 \text{ images}\cdot\text{s}^{-1}$.

Roughness

Surface roughness of EU and PI veneer samples were measured using a portable Handsurf profilometer (Accretech, Japan) unit consisting of main unit and pick-up. The stylus traverses the surface at a constant speed of $1,0 \text{ mm}\cdot\text{s}^{-1}$ over 12,5 mm. A total of 12 measurements evenly distributed were taken from the surface of each sample for Ra roughness measurements.

Plywood assembly

EU and PI veneers with an average thickness of $2,70 \text{ mm} \pm 0,07 \text{ mm}$ and $2,90 \text{ mm} \pm 0,7 \text{ mm}$, respectively, were carefully inspected and selected taking into account a uniform thickness, uniform surface and absence of wood defects, such as knots, cracks or imperfections caused by veneer machinery.

The lyophilized BSPC adhesive was dispersed in distilled water in 1: 6 and 1: 7 weight ratios and stirred for 10 minutes at $500 \text{ rad}\cdot\text{s}^{-1}$ at room temperature. A blue commercial food colorant was added to clearly distinguish the adhesive on wood surfaces.

Three ply plywoods were obtained with both woods, *Eucalyptus* and pine, using spread rates of $311 \text{ g}/\text{m}^2$ and $355 \text{ g}/\text{m}^2$ of wet adhesive in double glue line, with BSPC:water mass ratio 1:6 and 1:7, respectively (Liu and Li 2002). Pre-assembling time was 20 minutes. Hot press time, temperature and pressure were adjusted to 10 min, $140 \text{ }^\circ\text{C}$ and 1,5 MPa, respectively. Three samples of each conditions were made: *Eucalyptus* with 1:6 BSPC:water dispersion (EU 1:6), *Eucalyptus* with 1:7 BSPC:water dispersion (EU 1:7), pine with 1:6 BSPC:water dispersion (PI 1:6) and pine with 1:7 BSPC:water dispersion (PI 1:7). Each plywood was cut in 20 test specimens according to Argentinian norm IRAM 9562 (2006).

Plywood bond quality analysis

Plywoods bond quality analysis was measured according to Argentinian norm IRAM 9562 (2006). Test samples were divided into two groups, group A: samples without immersion treatment and group B: samples subject to a 24-hour water immersion treatment at room temperature.

Wood failure percentage was analyzed using an image software Image Pro (Media Cybernetics, USA).

Bond microanalysis

Microsections with a thickness of 30 μm to 35 μm were prepared from EU and PI plywoods after shear strength test, using a microtome. The area of interest for the microsections was that located between the two notches and the plane of sectioning was oriented parallel to the edge of the probe. The micro sections were taken in such way that they could show two successive wood veneers and the bond line between. Sections were stained with safranin (1 % v/v) and mounted into a microscope slide. Digital images were taken under a light microscope (Olympus CX31, Japan) attached to a digital camera (Infinity Lumenera, Canada). The images were then processed through specific software (ImagePro, Media Cybernetics, USA).

Statistical analysis

Experimental data were statistically analyzed using the one-way analysis of variance (ANOVA) along with Tukey's tests at 95 % confidence interval ($\alpha=0,05$).

RESULTS AND DISCUSSION

Rheological analysis of dispersed BSPC

The rheological behavior of BSPC with different water ratios was studied. Lyophilized adhesive was re-dispersed in distilled water in 1:10, 1:7, 1:6, 1:5, 1:4 ratios. Viscosity curves of all BSPC-based adhesives (Figure 1) follow a classic shear-thinning behavior (viscosity decreasing with increasing shear rate) as reported by Ciannamea *et al.* 2012). As expected, viscosities were higher in more concentrated dilutions, being much higher in 1:4 dispersions than the rest of them (two orders of magnitude higher than 1:5 dispersions). The apparent viscosity at low shear rate (1s^{-1} at 25 °C) of 1:10, 1:7, 1:6, 1:5 and 1:4 ratios was 5,25; 10,4; 35,9; 148 and 2400 Pa.s, respectively. There are three factors that an adhesive need to fulfill to form a proper bond: it must wet the surface, flow over and penetrate into the substrate without losing the adhesiveness between particles. An optimum penetration into the wood is considered essential for a good bond formation and this is partially dependent on the viscosity of the adhesive (Ciannamea *et al.* 2010). Adhesives must be fluid enough to flow into the microscopic holes, or capillary structure, of wood, but without causing over penetration.

Tests carried out, concluded that adhesives with viscosities 1: 4 and 1:5 were not feasible from a practical point of view, in accordance with (Kumar *et al.* 2002). High viscosity dispersions resulted too viscous to apply in veneers surfaces, resulting in insufficient penetration that can cause minimal surface contact for chemical bonding or "mechanical interlocking" (Chandler *et al.* 2005). On the other hand, test carried on with 1:10 dispersions resulted in too dilute to be applied on veneer's faces, producing over penetration. Therefore, dispersions of 1:6 and 1:7 were chosen to work with in further experiments.

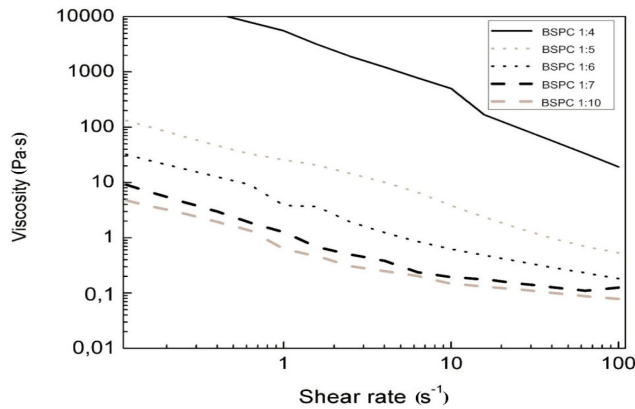


Figure 1: Viscosity as function of shear stress of soy bean adhesives.

Woods characterization

Density is a parameter that, apart from varying between species, varies within the same species and even within the same specimen (Calvo *et al.* 2006, Goche Télles *et al.* 2011). Both species show a great variation in wood density depending on the age of the trunk, being greater the older the specimen (Sánchez Acosta *et al.* 2005). For species of the same age, average density of UE is higher than the PI density.

The density of the *Eucalyptus* veneers was $0,54 \text{ g}\cdot\text{cm}^{-3} \pm 0,10 \text{ g}\cdot\text{cm}^{-3}$ with a moisture content of $9,4 \% \pm 0,15 \%$. Pine veneers presented a density of $0,52 \text{ g}\cdot\text{cm}^{-3} \pm 0,09 \text{ g}\cdot\text{cm}^{-3}$ with a moisture content of $8,6 \% \pm 0,5 \%$. The young age of the EU veneers, relative to the age of the PI veneers, may explain the low density in them and therefore the narrow range of densities between the two species.

Contact angle was measured for PI and EU using three different liquids which differ in polarity: diiodomethane, distilled water and glycerol. Figure 2 shows the equilibrium contact angle for PI and EU, while Table 1 shows the results of equilibrium contact angle and surface energies.

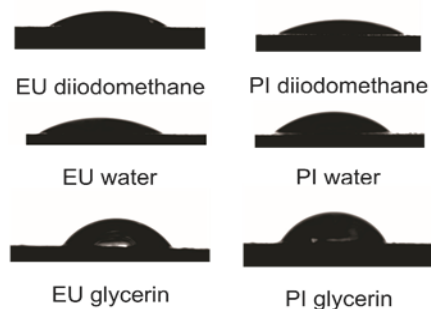


Figure 2: Equilibrium contact angle for (left) *Eucalyptus* and (right) pine.

Table 1: Surface energies and equilibrium contact angles for PI and EU.

Wood	γ	γ^d	γ^p	θ_{water}	$\theta_{\text{diiodomethane}}$	θ_{glycerin}
	$(\text{mJ}\cdot\text{m}^{-2})$					
PI	53,3	33,0	20,3	39 ± 3	34 ± 1	63 ± 7
EU	54,6	30,6	24,0	30 ± 3	35 ± 5	66 ± 7

During the initial phases of spreading and soaking of the drops, the change in contact angle was faster, getting slower towards the end of the process. A significant difference in the time necessary for the complete soaking of the drop could be seen between the solvents used, being quicker for diiodomethane, water, and the least for glycerin which can be related to increasing viscosity. Regardless PI or EU, equilibrium contact angles were higher for glycerin and no significant differences ($p > 0,05$) were found between diiodomethane and water equilibrium contact angles. Moreover, angles were no significant different between woods. Surface energies for PI and EU were also similar, being $53,3 \text{ mJ}\cdot\text{m}^{-2}$ for PI and slightly higher, $54,6 \text{ mJ}\cdot\text{m}^{-2}$, for EU.

The similarity between contact angle of PI and EU may be attributed to numerous reasons. In the first place the measurements were made in the tangential plane, perpendicular to the fiber's direction. Previous studies show greater variations in contact angle measurements in the radial plane where radial cells are exposed to the surface (Scheikl and Dunky 1998). Moreover, contact angles strongly depend on surface roughness (Papp and Csiha 2017) and in less amount among other parameters such as wood moisture, density and presence of extractives (Boehme and Hora 1996). Besides similar densities, both woods presented similar roughness, plus preconditioning moisture and temperature variables were the same for both. This explains the low differences in contact angles shown in Table 1.

Low water contact angles indicate a good wettability for both EU and PI with the SPC based adhesive (Aydin and Colakoglu 2007). From these results it is expected a good affinity between the adhesive and both woods, EU and PI. Therefore, any difference in the mechanical behavior between EU and PI plywoods may be attributable to morphology differences, rather than to affinity between wood and adhesive.

Bond quality analysis

The properties of the plywood were evaluated in terms of the bond quality test according to standard norm IRAM 9562 (2006). Tests were carried out both under dry conditions and after 24 hours of immersion in water at $20 \text{ }^\circ\text{C} \pm 3 \text{ }^\circ\text{C}$ (class 1: suitable for dry interior use). Besides the shear strength expressed in $\text{N}\cdot\text{mm}^{-2}$, another parameter that defines the quality of the bond is the percentage of wood fiber failure (WF %). A complete wood failure (100 % of wood fracture surface) indicates an excellent adhesion between veneers, which means that the measured strength is mainly determined by the strength of wood and not weakened by the presence of the joints between veneers. According to IRAM 9562 (2006), WF % values are determined visually by comparing with reference illustrations that show different percentages of wood failure. However, often it is not easy to visually estimate WF % values because with certain combinations of wood and adhesive, the wood failure area can only be detected in texture and generally requires a specific training (Plinke 2002). In order to clearly distinguish the fracture mode, a blue colorant was added to the adhesive which helps to identify the presence of adhesive in the fracture zone. In addition, an image processing software was used to detect, differentiate and measure the areas of adhesive and wood and determine the WF % with greater precision. Figure 3 shows the differences in fracture behavior of both PI and EU.

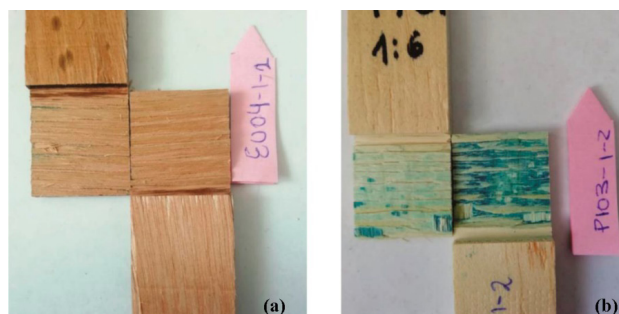


Figure 3: Fracture surface analysis. (a) *Eucalyptus* and (b) pine where the blue area corresponds to the exposed glued line.

Figure 4 shows the comparison of shear strength and WF % values under dry (group A) and wet conditions (group B). In all four cases, shear strength values decreased by at least 40 % after 24 h immersion. Wang *et al.* (2018) reported similar behavior when testing poplar and *Eucalyptus* veneers: shear strength of $0,82 \text{ N}\cdot\text{mm}^{-2} \pm 0,07 \text{ N}\cdot\text{mm}^{-2}$ had been reduced to $0,44 \text{ N}\cdot\text{mm}^{-2} \pm 0,08 \text{ N}\cdot\text{mm}^{-2}$ after immersion in water at $63 \text{ }^\circ\text{C}$ for 3 h.

No significant differences between 1:6 and 1:7 dispersions could be seen for PI and EU under dry conditions. PI 1:7 shear strength values in dry conditions were not significant different ($p < 0,05$) from EU samples tested in humid conditions evidencing the poor quality of PI unions with respect to EU ones. 1:6 PI values were even lower than 1:7 PI values. It is interesting to notice that WF % results are not susceptible to moisture content and adhesive solid content as there are no significant differences within EU probes and within PI samples (Figure 4).

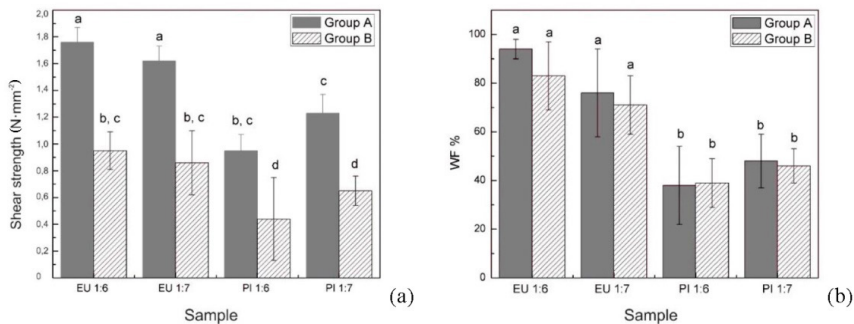


Figure 4: Comparison between A condition (dry) and B condition (wet) samples: (a) shear strength values (shear strength), (b) wood failure percentage values (WF %). Bars followed by different letters are significantly different ($p < 0,05$) by Tukey's Test.

IRAM 9562 (2006) standard establishes tolerance limits of WF % depending on the values of shear strength achieved. For example, if shear strength exceeds values of $1 \text{ N}\cdot\text{mm}^{-2}$, there are no restrictions in values of WF %. As shear strength values become lower, the proposed WF% limits become increasingly strict. In this way a shear strength vs. WF % graph is divided into an acceptable zone and a rejected zone as seen in Figure 6. Results of shear strength and WF % condition B samples are also shown in Figure 5. EU plywoods exhibit shear strength and WF % values around $1 \text{ N}\cdot\text{mm}^{-2}$ and over 70 %, respectively, being significantly higher than PI values. Results revealed better properties using 1:7 dispersions than 1:6 for EU and that both conditions were within the accepted region of the graph. Regarding PI results, the properties are significantly lower than EU, with PI 1:6 samples not accepted due to the qualities established in IRAM 9562 (2006) and PI 1:7 very close to the rejected region plus no significant differences were shown between them.

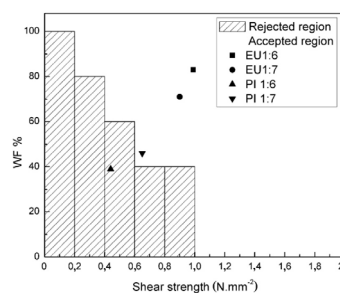


Figure 5: Relationship between wood failure percentage values (WF %) and shear strength for B condition samples (wet).

Bond line microscope analysis

This section intends to establish a relationship between the morphological and morphometric characteristics of each wood species used and the experimental response exposed above. The wood has mainly two cell systems, the axial and the radial system. The axial system has cells or rows of cells with their major axes oriented vertically, that is, parallel to the main axis of the trunk, while the radial system is formed by cells oriented horizontally in relation to the axis of the trunk. Each of these systems reveals an aspect of the wood morphology according to the type of cut being made: radial, tangential and transverse (Rowell 2012). In this study, when making a cross-section along the edge of the probe (between the notches), the inner veneer cells are cut in a radial plane and their smallest dimensions can be seen as shown in Figure 6. It should be noted that the adhesive penetration study was only carried out on the central face of the plywood since its fibers are oriented perpendicular to the direction of application of the force, being the veneer most prone to fail. In fact, the IRAM 9562 (2006) test is designed in such a way that the failure occurs through it.

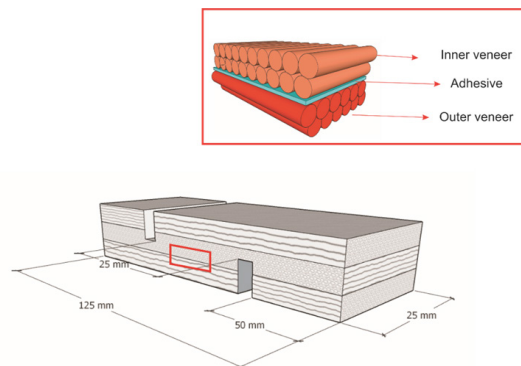


Figure 6: Scheme of IRAM 9562 (2006) samples dimensions and microsectioning area of bondline.

In this way, it is possible to see (and measure) characteristics such as the diameter of fibers, vessels, tracheid, parenchyma cells, vessel frequency, vessel area and vessels distribution among others, depending on whether it is PI or EU specie (Frihart and Hunt 2010). The single most important distinction between the two general kinds of wood is that EU (hardwood) have a characteristic type of cells call vessel elements (or pore) whereas PI (softwood) only presents tracheid in their axial system. These cells type have very different morphometry (diameter and length). The strength and quality of the union is expected to be intrinsically correlated to the way and degree of penetration of the adhesive in these different morphologies (Oliveira *et al.* 2020).

Figure 7 shows images 100x of both PI and EU morphological aspects of each type of wood axial system.

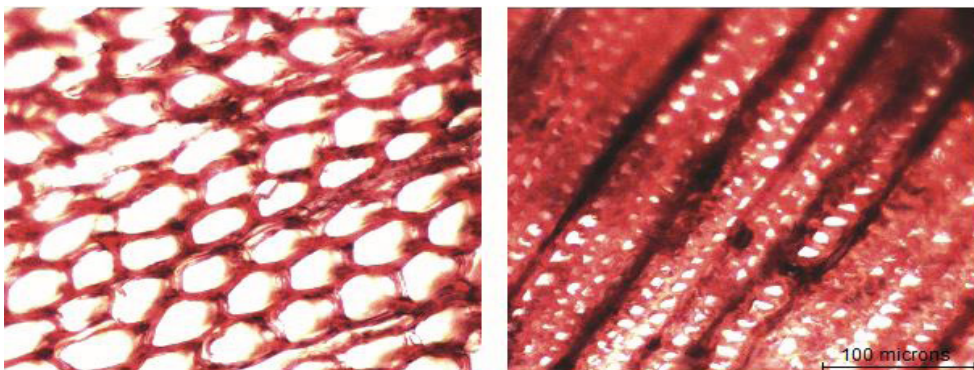


Figure 7: 100x wood images. Transverse section of earlywood tracheids (Left) pine and (Right) *Eucalyptus* fibers.

EU fiber lumen diameter average was $13 \mu\text{m} \pm 4 \mu\text{m}$, in accordance with Monteoliva *et al.* (2015) measurements for *Eucalyptus grandis* species of Argentina. PI earlywood lumen average was $26 \mu\text{m} \pm 7 \mu\text{m}$. The greatest difference between both cell structures is in the relationship between the width of the cell wall and the diameter of the lumen, being greater in the earlywood tracheids, making them more likely to be crushed and weakened by unwinding processes or pressing stages than *Eucalyptus* fibers, or at least the damage is greater. In addition, when aqueous adhesives are used, the cells close to the glue line can reach a high moisture content. In these conditions these cells, especially in earlywood, are more likely to buckle during pressing (Hunt *et al.* 2018).

Figure 8 shows the bondline of a PI sample and the deformation or rupture of earlywood tracheids next to the bondline. Broken or crushed in the surface cells might increase the potentiality of failure through the bondline in PI samples and it might be one reason for the difference in WF % values between PI and EU presented in the previous section.

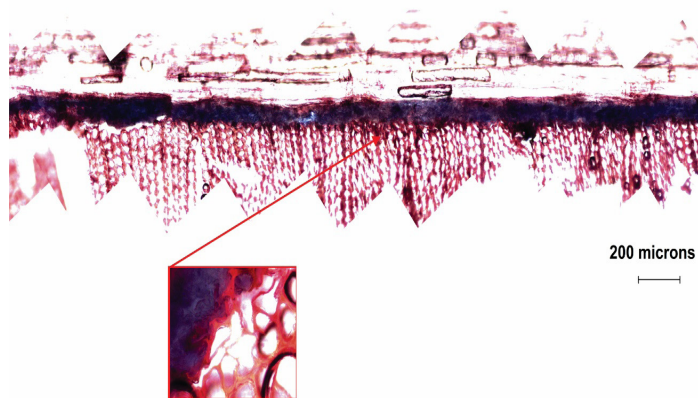


Figure 8: Tracheids deformation close to the bondline in PI samples.

It is known that the presence of vessels weakens the strength of wood. However, the vessels present in EU that are exposed to the veneers surface are filled with adhesive and act as points where mechanical interlocking is enhanced providing additional shear strength (Frihart 2005). Moreover, the surface contact area between the adhesive and the cell wall increases considerable at these points (vessels). Contact area is directly related to adhesion force due to covalent bonding and formation of secondary chemical bonds increasing resistance to debonding (Kamke and Lee 2007). At these points, the average thickness of the glue line increases by almost 200 % as can be seen in Figure 9. On the contrary, the unfilled vessels located within the central part of plywood are weak zones prone to break under shear stress load. It is worth noting the absence of tylose and deposits in this *Eucalyptus* vessels which could partially or completely block the vessel lumen.

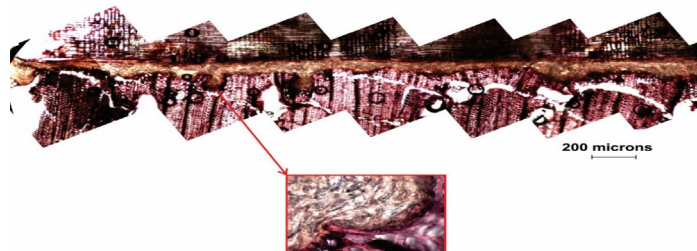


Figure 9: *Eucalyptus* bond line. Vessels filled with adhesive act as mechanical interlocking and contact area between adhesive and wood is increased.

Also, by analyzing the samples's cross-sectional profile, it can be seen that the fracture extends with a constant profile across the entire width of the sample, as reported by other authors for birch plywood samples particularly when tested with lathe checks pulled closed (Rohumaa *et al.* 2013, Hunt *et al.* 2018). The latter could be related not only to the presence of lathe checks but also to the diagonal arrangement of the vessels oriented 45° with respect to the load as it is shown in Figure 10.

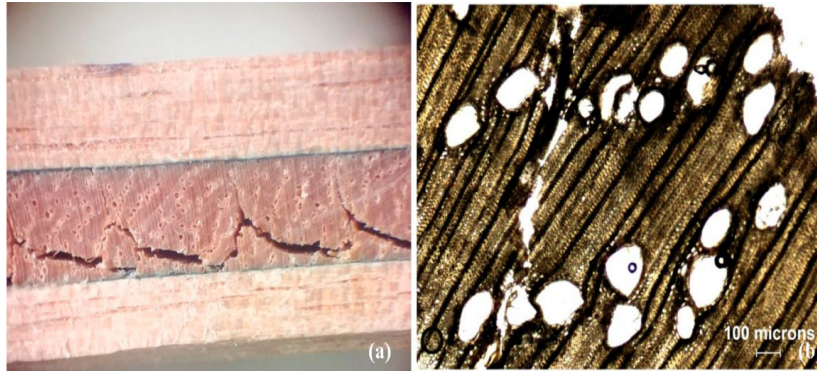


Figure 10: (a) Serrate profile fracture in EU wood (macroscopic image 10x) and (b) empty EU vessels with diagonal pattern from interior of plywood (microscopic image 40x).

CONCLUSIONS

The performance of the biobased BSPC adhesive was excellent for *Eucalyptus* plywood accomplishing IRAM 9562 (2006) standards for interior use class I. No significant differences were found between 1:6 and 1:7 dispersions.

PI plywoods showed low values of shear strength and %WF. 1:7 adhesive dispersion barely accomplishing norm IRAM 9562 (2006) while 1:6 dispersion failed it.

A relationship could be established between the WF% values and the morphological aspect of each type of wood. Broken or crushed tracheids in pine enhance debonding between veneers giving lower values of WF%, whereas the presence and diagonal arrangement of vessels in EU wood can act as weak links contributing to determine the path of fracture propagation through the central veneer.

ACKNOWLEDGEMENTS

The authors acknowledge the financial support from CONICET (National Scientific and

Technical Research Council) and National Agency of Promotion of Science and Technology (ANPCyT) grand number PICT 2016-0445.

REFERENCES

Ang, A.F.; Ashaari, Z.; Lee, S.H.; Tahir, P.M.; Halis, R. 2019. Lignin-based copolymer adhesives for composite wood panels-A review. *Int J Adhes Adhes* 95: 102408. <https://doi.org/10.1016/j.ijadhadh.2019.102408>

ASA. 2020. Soy stats Report. United States. https://soygrowers.com/wp-content/uploads/2020/05/SoyStats2020_for-WEB.pdf

Aydin, I.; Colakoglu, G. 2007. Variation in surface roughness, wettability and some plywood properties after preservative treatment with boron compounds. *Build Environ* 42(11): 3837-3840. <https://doi.org/10.1016/j.buildenv.2006.11.009>

Boehme, C.; Hora, G. 1996. Water absorption and contact angle measurement of native European, North American and tropical wood species to predict gluing properties. *Holzforschung* 50(3): 269-276. <https://doi.org/10.1515/hfsg.1996.50.3.269>

Buddi, T.; Mahesh, K.; Muttill, N.; Rao, B.N.; Nagalakshmi, J.; Singh, S.K. 2017. Characterization of plywoods produced by various bio-adhesives. *Mater Today* 4(2): 496-508. <https://doi.org/10.1016/j.mat-pr.2017.01.050>

Bulfe, N.M.L.; Fernández, M.E. 2017. Anatomía funcional del leño juvenil de *Pinus taeda* L: variabilidad genotípica y plasticidad anatómica ante déficit hídrico. *Revista de la Facultad de Agronomía, La Plata* 116(2): 225-240. <https://revistas.unlp.edu.ar/revagro/article/view/6177>

Calvo, C.F.; Cotrina, A.; Cuffré, A.G.; Piter, J.; Stefani, P.M.; Torrán, E.A. 2006. Variación radial y axial del hinchamiento, del factor anisotrópico y de la densidad, en el *Eucalyptus grandis* de Argentina. *Maderas-Cienc Tecnol* 8(3):159-168. <http://dx.doi.org/10.4067/S0718-221X2006000300003>

Ciannamea, E.; Martucci, J.; Stefani, P.; Ruseckaite, R. 2012. Bonding Quality of Chemically-Modified Soybean Protein Concentrate-Based Adhesives in Particleboards from Rice Husks. *J Am Oil Chem Soc* 89(9): 1733-1741. <https://doi.org/10.1007/s11746-012-2058-2>

Ciannamea, E.M.; Marin, D.; Ruseckaite, R.A.; Stefani, P. M. 2017. Particleboard Based on Rice Husk: Effect of Binder Content and Processing Conditions. *J Renew Mater* 5(5): 357-362. <https://doi.org/10.7569/JRM.2017.634125>

Ciannamea, E.M.; Stefani, P.M.; Ruseckaite, R.A. 2010. Medium-density particleboards from modified rice husks and soybean protein concentrate-based adhesives. *Bioresour Technol* 101(2): 818-825. <https://doi.org/10.1016/j.biortech.2009.08.084>

Chalapud, M.C.; Herdt, M.; Nicolao, E.S.; Ruseckaite, R.A.; Ciannamea, E.M.; Stefani, P.M. 2020. Biobased particleboards based on rice husk and soy proteins: Effect of the impregnation with tung oil on the physical and mechanical behavior. *Constr Build Mater* 230: 116996. <https://doi.org/10.1016/j.conbuildmat.2019.116996>

Chandler, J.G.; Brandon, R.L.; Frihart, C.R. 2005. Examination of adhesive penetration in modified wood using fluorescence microscopy. ASCS Spring 2005 Convention and Exposition: April 17-20, Columbus, OH. (Bethesda, Md.: Adhesive and Sealant Council, 2005): 10 p. <https://www.fs.usda.gov/treesearch/pubs/23115>

Denne, M.P. 1989. Definition of latewood according to Mork (1928). *IAWA J* 10(1): 59-62. <https://doi.org/10.1163/22941932-90001112>

FAO. 2018. FAOSTAT. Food and Agriculture Organization of the United Nations: Rome, Italy. <http://www.fao.org/faostat>

Frihart, C.R. 2005. Adhesive bonding and performance testing of bonded wood products. In *Advances in Adhesives, Adhesion Science, and Testing*. Damico, D. (ed.), West Conshohocken, PA: USA. ASTM International. 1-12. <https://doi.org/10.1520/STP11654S>

Frihart, C.R.; Hunt, C.G. 2010. *Wood handbook: wood as an engineering material*. General technical report FPL; GTR-190. Centennial ed: Madison, WI. US Dept. of Agriculture, Forest Service, Forest Products Laboratory. https://www.fpl.fs.fed.us/documnts/fplgtr/fpl_gtr190.pdf

Frihart, C.R.; Birkeland, M.J. 2014. Soy properties and soy wood adhesives. In: Brentin RP, editor. *Soy-based chemicals and materials*. Washington (DC): American Chemical Society. p. 167-192. <https://doi.org/10.1021/bk-2014-1178.ch008>

Ghahri, S.; Chen, X.; Pizzi, A.; Hajihassani, R.; Papadopoulos, A.N. 2021. Natural Tannins as New Cross-Linking Materials for Soy-Based Adhesives. *Polymers* 13(4): 595. <https://doi.org/10.3390/polym13040595>

Goche Télles, J.R.; Velázquez Martínez, A.; Borja de la Rosa, A.; Capulín Grande, J.; Palacios Mendoza, C. 2011. Variación radial de la densidad básica en *Pinus patula* Schltdl. et Cham. de tres localidades en Hidalgo. *Rev Mex Cienc Forestales* 2(7): 71-78. http://www.scielo.org.mx/scielo.php?script=sci_arttext&pid=S2007-11322011000500006

Hunt, C.G.; Frihart, C.R.; Dunky, M.; Rohumaa, A. 2018. Understanding wood bonds-going beyond what meets the eye: a critical review. *Reviews of Adhesion and Adhesives* 6(4): 369-440. <https://doi.org/10.7569/RAA.2018.097312>

IRAM. 2006. Determinación de la calidad de encolado. IRAM 9562. 2006. Buenos Aires, Argentina.

IRAM. 1963. Método de determinación de la humedad. IRAM 9532. 1963. Buenos Aires. Argentina.

IRAM. 1973. Método de determinación de la densidad aparente. IRAM 9544. 1973. Buenos Aires. Argentina.

Jakes, J.E.; Frihart, C.R.; Hunt, C.G.; Yelle, D J.; Plaza, N.Z.; Lorenz, L.; Grigsby, W.; Ching, D.J.; Kamke, F.; Gleber, S.C. 2019. X-ray methods to observe and quantify adhesive penetration into wood. *J Mater Sci* 54(1): 705-718. <https://doi.org/10.1007/s10853-018-2783-5>

Kamke, F.A.; Lee, J.N. 2007. Adhesive penetration in wood-a review. *Wood Fiber Sci* 39(2): 205-220. <https://wfs.swst.org/index.php/wfs/article/view/641>

Kumar, R.; Choudhary, V.; Mishra, S.; Varma, I.K.; Mattiason, B. 2002. Adhesives and plastics based on soy protein products. *Ind Crop Prod* 16(3): 155-172. [https://doi.org/10.1016/S0926-6690\(02\)00007-9](https://doi.org/10.1016/S0926-6690(02)00007-9)

Liu, Y.; Li, K. 2002. Chemical modification of soy protein for wood adhesives. *Macromol Rapid Commun* 23(13): 739-742. [https://doi.org/10.1002/1521-3927\(20020901\)23:13<739::AID-MARC739>3.0.CO;2-0](https://doi.org/10.1002/1521-3927(20020901)23:13<739::AID-MARC739>3.0.CO;2-0)

Marra, A.A. 1992. *Technology of wood bonding: principles in practice*. Van Nostrand: New York, United States.

Mo, X.; Sun, X.S. 2013. Soy proteins as plywood adhesives: formulation and characterization. *J Adhes Sci Technol* 27(18-19): 2014-2026. <https://doi.org/10.1080/01694243.2012.696916>

Monteoliva, S.; Barotto, A.J.; Fernandez, M.E. 2015. Anatomía y densidad de la madera en *Eucalyptus*: variación interespecífica e implicancia en la resistencia al estrés abiótico. *Rev Fac Agro* 114(2): 209-217. <http://revista.agro.unlp.edu.ar/index.php/revagro/article/view/130>

Nicolao, E.; Leiva, P.; Chalapud, M.; Ruseckaite, R.; Ciannamea, E.; Stefani, P. 2020. Flexural and tensile properties of biobased rice husk-jute-soybean protein particleboards. *J Build Eng* 101261. <https://doi.org/10.1016/j.jobe.2020.101261>

Nordqvist, P.; Nordgren, N.; Khabbaz, F.; Malmström, E. 2013. Plant proteins as wood adhesives: Bonding performance at the macro-and nanoscale. *Ind Crops Prod* 44: 246-252. <https://doi.org/10.1016/j.indcrop.2012.11.021>

Oliveira de, R.G.; Gonçalves, F.G.; Segundinho, P.G. de A.; Oliveira, J.T. da S.; Paes, J. B; Chaves, I.L.; Brito, A.S. 2020. Analysis of glue line and correlations between density and anatomical characteristics of *Eucalyptus grandis* × *Eucalyptus urophylla* glulam. *Maderas-Cienc Tecnol* 22(4): 495-504. <http://dx.doi.org/10.4067/S0718-221X2020005000408>

Papp, E.A.; Csiha, C. 2017. Contact angle as function of surface roughness of different wood species. *Surf Interfaces* 8: 54-59. <https://doi.org/10.1016/j.surfin.2017.04.009>

Piter, J.; Cotrina A.; Zitto, M.S.; Stefani, P.M.; Torrán, E. 2007. Determination of characteristic strength and stiffness values in glued laminated beams of Argentinean *Eucalyptus grandis* according to European standards. *Holz Roh Werkst* 65(4): 261-266. <https://doi.org/10.1007/s00107-006-0161-5>

Pizzi, A. 2006. Recent developments in eco-efficient bio-based adhesives for wood bonding: opportunities and issues. *J Adhes Sci Technol* 20(8): 829-846. <https://doi.org/10.1163/156856106777638635>

Plinke, B. 2002. Automatic determination of wood fibre failure percentage of plywood shear samples Wood based materials. In Wood composites and chemistry : International symposium, September 19-20, 2002. Vienna, Austria, p.247-256 <http://publica.fraunhofer.de/documents/N-15521.html>

Rohumaa, A.; Hunt, C.G.; Hughes, M.; Frihart, C.R.; Logren, J. 2013. The influence of lathe check depth and orientation on the bond quality of phenol-formaldehyde-bonded birch plywood. *Holzforschung* 67(7): 779-786. <https://doi.org/10.3390/polym13040595>

Rowell, R.M. 2012. *Handbook of wood chemistry and wood composites*. CRC press: United States.

Salthammer, T.; Mentese, S.; Marutzky, R. 2010. Formaldehyde in the indoor environment. *Chem Rev* 110(4): 2536-2572. <https://doi.org/10.1021/cr800399g>

Sánchez Acosta, M.; Zakowicz, N.; Harrand, L.; Cuffre, A.; Torran, E.; Calvo P.J. 2005. Propiedades físicas mecánicas de la madera de *Eucalyptus grandis* de las procedencias genéticas: Kendall (Australia), Huerto semillero de Sudáfrica y semilla local Concordia, plantadas comercialmente en Argentina. In *Congreso Mundial IUFRO*. Entre Rios, Argentina.

Scheickl, M.; Dunky, M. 1998. Measurement of dynamic and stau contact angles on wood for the determination of its surface tension and the penetration of liquids into the wood surface. *Holzforschung* 52(1): 89-94. <https://doi.org/10.1515/hfsg.1998.52.1.89>

Stefani, P.M.; Peña C.; Ruseckaite, R.A.; Piter, J.; Mondragon, I. 2008. Processing conditions analysis of *Eucalyptus globulus* plywood bonded with resol-tannin adhesives. *Bioresour Technol* 99(13): 5977-5980. <https://doi.org/10.1016/j.biortech.2007.10.013>

Vázquez, G.; Galinanes, C.; Freire, M.S.; Antorrena, G.; González-Alvarez, J. 2011. Wettability study and surface characterization by confocal laser scanning microscopy of rotary-peeled wood veneers. *Maderas-Cienc Tecnol* 13(2): 183-192. <https://doi.org/10.4067/S0718-221X2011000200006>

Wang, F.; Wang, J.; Chu, F.; Wang, C.; Jin, C.; Wang, S.; Pang, J. 2018. Combinations of soy protein and polyacrylate emulsions as wood adhesives. *Int J Adhes Adhes* 82: 160-165. <https://doi.org/10.1016/j.ijadhadh.2018.01.002>

Wolkenhauer, A.; Avramidis, G.; Hauswald, E.; Militz, H.; Viöl, W. 2009. Sanding vs. plasma treatment of aged wood: A comparison with respect to surface energy. *Int J Adhes Adhes* 29(1): 18-22. <https://doi.org/10.1016/j.ijadhadh.2007.11.001>

Xi, X.; Pizzi, A.; Frihart, C.; Lorenz, L.; Gerardin, C. 2020. Tannin plywood bioadhesives with non-volatile aldehydes generation by specific oxidation of mono-and disaccharides. *Int J Adhes Adhes* 98: 102499. <https://doi.org/10.1016/j.ijadhadh.2019.102499>